In-vivo detection of cell cycle arrest using manganese-enhanced MRI (MEMRI)

S. Saito[1], S. Hasegawa[1], T. Furukawa[1], T. Saga[1], and I. Aoki[1]
[1]Molecular Imaging Center (MIC), National Institute of Radiological Sciences (NIRS), Chiba, Chiba, Japan

INTRODUCTION

Recent studies on the utility of manganese have shown that manganese-enhanced MRI (MEMRI) can detect cellular alterations in tumor models [1][2]. In addition, the intercellular contrast agent $MnCl_2$ has been successfully used to assess cell viability in heart ischemia [3], and cells can be easily labeled using Mn^{2+} in vitro [4]. Hasegawa et al. reported that MEMRI can reflect MnSOD over-expression in a tumor model [2]. Radiotherapy using high-energy x-rays treats malignancies with the intention of destroying or inactivating cells while preserving normal tissue integrity. We investigated the relationship between x-ray irradiation and Mn uptake in tumor cells and tested whether MEMRI can detect radiation-induced cell disturbances at an early stage both in vitro and in vivo.

MATRIALS AND METHODS

X-ray irradiation:
Colon26 cells (1 day before the MRI scan) and tumor- bearing mice (7 days after tumor detection) were exposed to a single dose of 20 Gy of X-ray irradiation. The X-ray irradiation conditions were 200 kVp, 20 mA, 0.5 mm Cu + 0.5 mm Al filter, 500 mm distance from focus to object and a dose rate of 1.3 Gy/min.

In vitro MEMRI: Normal and X-ray irradiated (24 h after irradiation) cells were incubated with medium containing $MnCl_2$ (0.1 mM) for 30 min at 37°C under 5% CO_2 and the medium then removed by careful washing with phosphate-buffered saline (PBS). The cells were harvested, transferred to a 96-well PCR tube, and pelleted by centrifugation. MRI was performed using a 7.0-T unit (Kobelco and Jastec, Japan). A 30-mm inner-diameter mice volume coil (Rapid Biomedical, Germany) was used for measurement of cell samples. The measurements were performed using T_1-weighted MRI (T_1WI) with a conventional spin echo (SE) sequence (TR, 400 ms; echo time, TE, 9.57 ms; matrix size, 256 × 256; field of view (FOV), 51.2 × 51.2 mm^2; slice thickness, 1.0 mm; fat suppression, on; and number of acquisitions (NA), 8). Inversion recovery imaging using RARE was used for T_1 calculations (TR, 10000 ms; TE, 10 ms; inversion time, 51, 100, 200, 400, 800, 1600, 3200, or 6400 ms; matrix size, 128 × 128; FOV, 51.2 × 51.2 mm^2; RARE factor, 4). Quantitative T_1 maps were calculated using non-linear least square fitting using inversion recovery MRI. Regions of interest (ROI) were defined as the precipitated cell region. For evaluation of manganese uptake, we used the relaxation rate (R_1), which is the inverse of T_1 ($R_1 = 1/T_1$). All calculations and analyses were performed using MRVision image analysis software (Version 1.5.8, MRVision Co.). **Flow cytometry:** Cell viability and cell cycle alterations were measured using Guava Viacount reagent and a Guava PCA machine (Guava Technologies Inc., Hayward, CA, USA). Normal and X-ray irradiated (24 h later after irradiation) cells were plated in 6-well plates. Cells were then analyzed on a Guava PCA machine using the Viacount Acquisition Module. **In vivo MEMRI animal models**: Subcutaneous tumor models were formed on both sides of the lower backs of 14 nude mice (Japan SLC, N = 6 for MRI scanning, N = 8 for tumor size measurement) by subcutaneous injection of 1×10^7 colon26 cells in 100 µl of PBS buffer. Two perpendicular tumor diameters were measured with a caliper on days 1, 3 and 7 after radiation exposure. Tumor volumes were calculated as $V = (\pi/6) \times a\ (mm) \times b\ (mm^2)$, with a and b being the largest and smallest perpendicular tumor diameters, respectively. Subsequent measurements were normalized to pretreatment tumor volume. The 6 mice were anesthetized with 1.5-2.0% isoflurane and placed in the prone position. T_1WI acquisitions were performed in the following order: the pre-administration (control), the Gd-enhanced, and the Mn-enhanced experiments. First, one T_1WI image was acquired as the control before Gd administration. Second, T_1WI acquisition was repeated twice every 16 min after Gd-DTPA administration. Gd-DTPA (150 µmol/kg, Bayer Japan, Japan) was diluted to 50 mM with saline and injected intravenously to evaluate tumor vasculature condition. Third, T_1WI acquisition was repeated 4 times every 32 min after the start of Mn^{2+} infusion. We slowly infused the 50 mM osmotic pressure-controlled $MnCl_2$ solution (380 µmol/kg) at a rate of 4.0 ml/h through the tail vein using a syringe pump for 30 min. For T_1WI imaging of subcutaneous tumors, 2D single-transversal slice T_1WI was obtained using a conventional SE sequence with the following parameters: TR, 400 ms; TE, 9.57 ms; matrix size, 256 × 256; FOV, 40.0 × 40.0 mm^2; slice thickness, 1.0 mm; fat suppression, on; and NA, 4. T_2-mappings were acquired using a multi-slice multi-echo SE sequence (TR, 3000 ms; slice thickness, 1 mm; FOV, 40.0 × 40.0 mm; matrix, 128 × 128; slice orientation, transaxial; number of repetitions, 1) with echo-times ranging from 10 to 140 ms in steps of 10 ms. All tumors were extracted for histology after MRI. Tumor sections were stained with Cyclin-D1, Ki-67, Activated Caspase-3 and Laminin.

RESULTS and DISCUSSION

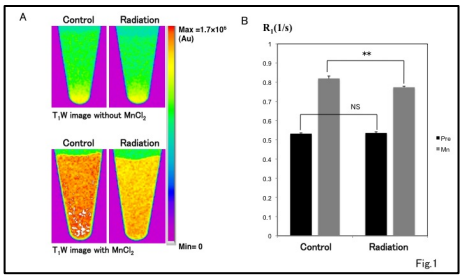

Fig.1

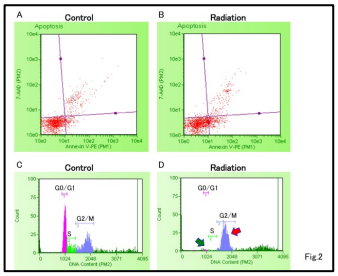

Fig.2

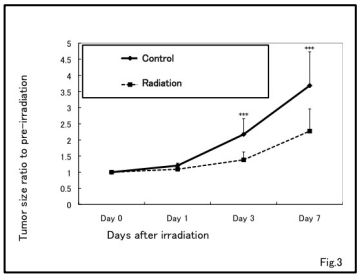

Fig.3

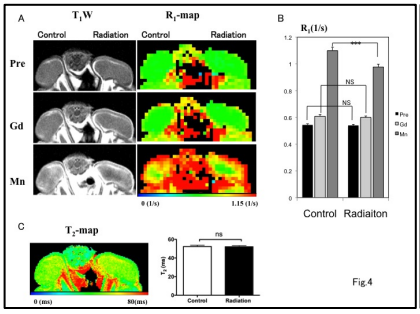

Fig.4

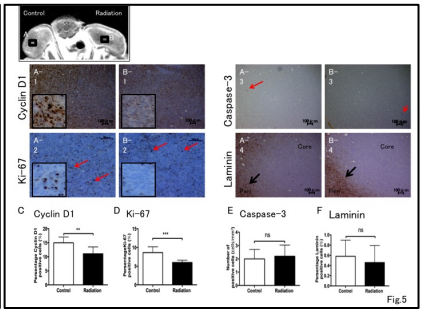

Fig.5

Figure 1A shows T_1WI imaging of the cell pellets of control and X-ray irradiated colon26 cells when incubated with standard medium supplemented without (left upper low) or with (left bottom low) 0.1 mM $MnCl_2$. We found that x-ray irradiated colon26 cells had a lower T_1 signal compared to normal colon26 cells enhanced with 0.1 mM $MnCl_2$. **Figure 1B** shows the R_1 value of cells. The decrease in the R_1 values of x-ray irradiated colon26 cells was more apparent than that of the control colon26 cells enhanced with 0.1 mM $MnCl_2$. **Figure 2** shows the flow cytometry results. The Annexin V assay distinguished among early apoptosis, late apoptosis, and an apoptotic or necrotic phase in which the cells were labeled with both Annexin V and 7-ADD. The apoptosis of x-ray irradiated cells can be detected (right upper graph). The cell cycle was detected using DNA content flow cytometry. G2/M phase cells showed increased numbers among the irradiated colon26 cells (red arrow). **Figure 3** shows tumor growth in radiation-treated and control mice. Tumor growth in the mice was significantly lower after 3 and 7 days exposure to radiation ($P<0.001$). **Figure 4A** shows T_1WI and R_1-map data of the x-ray treated and control tumors. **Figure 4B** shows that the R_1 values were lower in the radiation-exposed tumors after 24 h. **Figure 4C** shows a T_2-map of the x-ray treated and control tumors. There were no differences between the two tumor groups. **Figures 5A~F** show the histological results 24 h after treating the tumors with x-ray irradiation. The numbers of Cyclin-D1 and Ki-67 stained cells were lower among the irradiated colon26 tumors. **CONCLUSIONS** Manganese-enhanced MRI is able to detect cell cycle arrest of tumor cells following radiation exposure. Reductions in Mn accumulation in the irradiated cells were observed both in vitro and in vivo. MEMRI may be suitable for evaluation of not only cell viability but also the acute stage of cell cycle alteration after radiotherapy.

REFERENCES [1] Seshadri M. MRM; 2010 [2] Hasegawa S. IJC; 2010 [3] Tom C.- C. Hu. MRM; 2005 [4] Ichio Aoki. NMR in biomedicine; 2006.